Supplementary Information for: CASP15 cryo-EM protein and RNA targets: refinement and analysis using experimental maps

- Thomas Mulvaney[1,2] https://orcid.org/0000-0002-4373-6160
- Rachael C. Kretsch[3] https://orcid.org/0000-0002-6935-518X
- Luc Elliott[4] https://orcid.org/0009-0002-0181-4041
- Joseph G. Beton[1] https://orcid.org/0000-0001-7499-3867
- Andriy Kryshtafovych[5] https://orcid.org/0000-0001-5066-7178
- Daniel J. Rigden[4] https://orcid.org/0000-0002-7565-8937
- Rhiju Das[3,6,7] https://orcid.org/0000-0001-7497-0972
- Maya Topf[1,2] https://orcid.org/0000-0002-8185-1215

1. Centre for Structural Systems Biology (CSSB), Leibniz-Institut für Virologie (LIV),
2. University Medical Center Hamburg-Eppendorf (UKE), Hamburg,
3. Biophysics Program, Stanford University School of Medicine, CA USA
4. Institute of Systems, Molecular & Integrative Biology, The University of Liverpool, UK
5. Genome Center, University of California, Davis, Davis, California, USA
6. Department of Biochemistry, Stanford University School of Medicine, CA USA
7. Howard Hughes Medical Institute, Stanford University, CA USA

Correspondence to be sent to: maya.topf@cssb-hamburg.de

Supplemental Methods

1 | Refinement pipeline

As per the CASP13 and CASP14 modeling experiments[1,2], predictions of cryoEM targets were positioned in the density by using a ChimeraX script. The script aligned predictions to the reference model using the 'matchmaker' command and then optimized the local fit to the experimental map using the 'fitmap' function. The fitting and refinement stages of the pipeline **(Fig. S1)** used a hierarchical approach built on our previous protocol designed for Flex-EM/RIBFIND[3]. This approach was previously shown to allow large conformational changes to take place and avoid trapping parts of the model in small density pockets during fitting. The TEMPy-ReFF software package[4] supports this hierarchical approach by automatically breaking down clusters as refinement progresses. This package offers a number of force-fields and routines for building pipelines for fitting and refinement using the OpenMM molecular dynamics engine [5]. In our application of the software here **(Fig. S1),** the models were iteratively broken down into smaller rigid-bodies using the RIBFIND2 software[6]. These subunits were composed of interacting secondary structure elements determined using DSSP[7] for proteins and RNAView[8] for RNA. Each subunit was then subjected to a fitting force which is simply the negative gradient of the cryoEM map[9], whilst strong harmonic restraints maintain the overall geometry of the subunit.

In the last stage, the models were refined using a Gaussian mixture model (GMM)-based potential similar to the component-based approach of[10], but this time applied to atoms. In this scheme, each atom is represented by a Gaussian where the mean is given by the atom's position, sigma can intuitively be thought of as its resolution or Bfactor, and the height is the atomic number that approximates the scattering potential of neutral atoms. Using the expectation-maximization algorithm for GMMs, the atomic positions are successively updated so

as to maximize the likelihood that the Gaussians represent the experimental data while at the same time, an AMBER14 force-field[11] corrects stereo-chemistry. A simulated map represented by a GMM can be described by the following equation where M_{sim} is a simulated map, N is the number of atoms in the atomic model, v is a voxel and x_i, B_i and Z_i are the position, Bfactor and atomic numbers of the i^{th} atom respectively:

$$M_{sim}(v) = \sum_{i}^{N} \frac{Z_i}{B_i^3} exp(-\frac{|v - x_i|^2}{2B_i^2})$$

Despite the RIBFIND rigid body restraints, early testing of the pipeline showed that some RNA models suffered from distortions. Therefore, our final protocol included an additional stage of corrections using the ERRASER2 program, an unpublished accelerated version of the ERRASER protocol for the refinement of RNA in crystallographic and cryoEM maps[12]. It is available as part of the ROSETTA package[13]. However, here ERRASER2 was used only for optimisation of the structure and not the fit to the density before final refinement of the structure using the GMM (see Listing 1).

2 | Choice of docking software for chain ranking

A Spearman rank correlation coefficient was performed to compare the rankings produced by Molrep and PowerFit. For the majority of cryo-EM targets there were no significant differences between the PowerFit and Molrep rankings. However, for a minority of cryo-EM targets, significant differences were seen. The greatest differences were for T1114s3 (PowerFit median CC: 0.6483, Molrep median CC: 0.587), T1137s1 (PowerFit CC: 0.17285, Molrep CC: 0.12070), T1137s3 (PowerFit CC: 0.1894, Molrep CC: 0.1273), T1137s5 (PowerFit CC: 0.20345, Molrep CC: 0.11065), T1157s1 (PowerFit CC: 0.46999˙, Molrep CC: 0.6101) and T1185s1 (PowerFit

CC: 0.317, Molrep CC: 0.439). Since PowerFit outperformed Molrep in those cases more often than the reverse, PowerFit's placements were chosen for the rankings.

Supplementary Tables

Target	Group	(o)lDDT		GDT-TS score		QS-score		TM score	
		Pred.	Refined	Pred.	Refined	Pred.	Refined	Pred.	Refined
T1154	494	0.84	0.77	0.63	0.78	NA	NA	NA	NA
T1158	367	0.84	0.86	0.64	0.92	NA	NA	NA	NA
T1169	466	0.66	0.67	0.53	0.72	NA	NA	NA	NA
H1157	239	0.66	0.7	NA	NA	0.67	0.8	0.78	0.80
T1170o	165	0.70	0.85	NA	NA	0.61	0.85	0.90	0.90
T1121o	091	0.74	0.69	NA	NA	0.31	0.25	0.66	0.64

Table S1: Predictions which ranked high by docking but did not pass CASP scoring criteria: Values for TM, GDT-TS, (o)lDDT and QS scores of predictions and their respective refined models. TM and QS scores were not applicable to monomeric targets.

Supplemental Figures

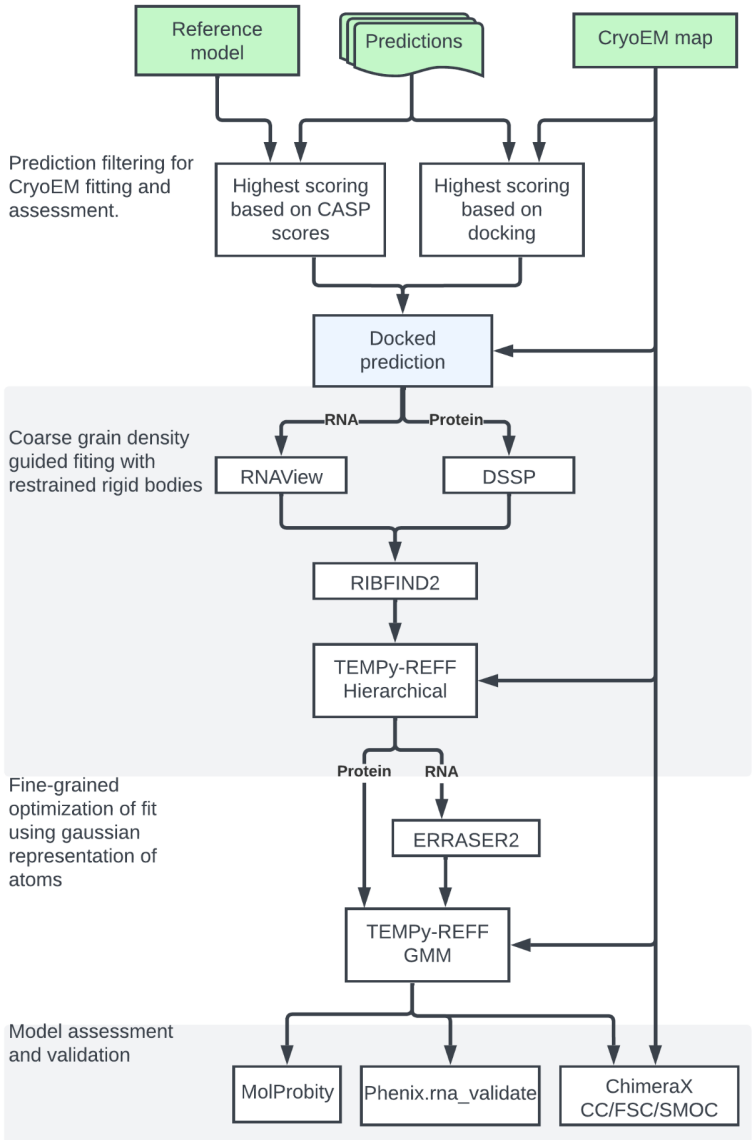

Fig. S1: Docking and refinement pipeline. Submitted predictions were chosen for cryo-EM refinement based on CASP metrics (using the reference structure) and using a ranking scheme which assesses the overall fit of predictions constituent chains to the experimental map. Selected models are then flexibly fit to the experimental data using a coarse-grained hierarchical fitting protocol. Corrections were made to RNA model geometry using ERRASER2 followed by an atomistic refinement scheme based using TEMPy-ReFF. Models were then assessed using MolProbity, Phenix.rna_validate, ChimeraX CC and TEMPy SMOC scores.

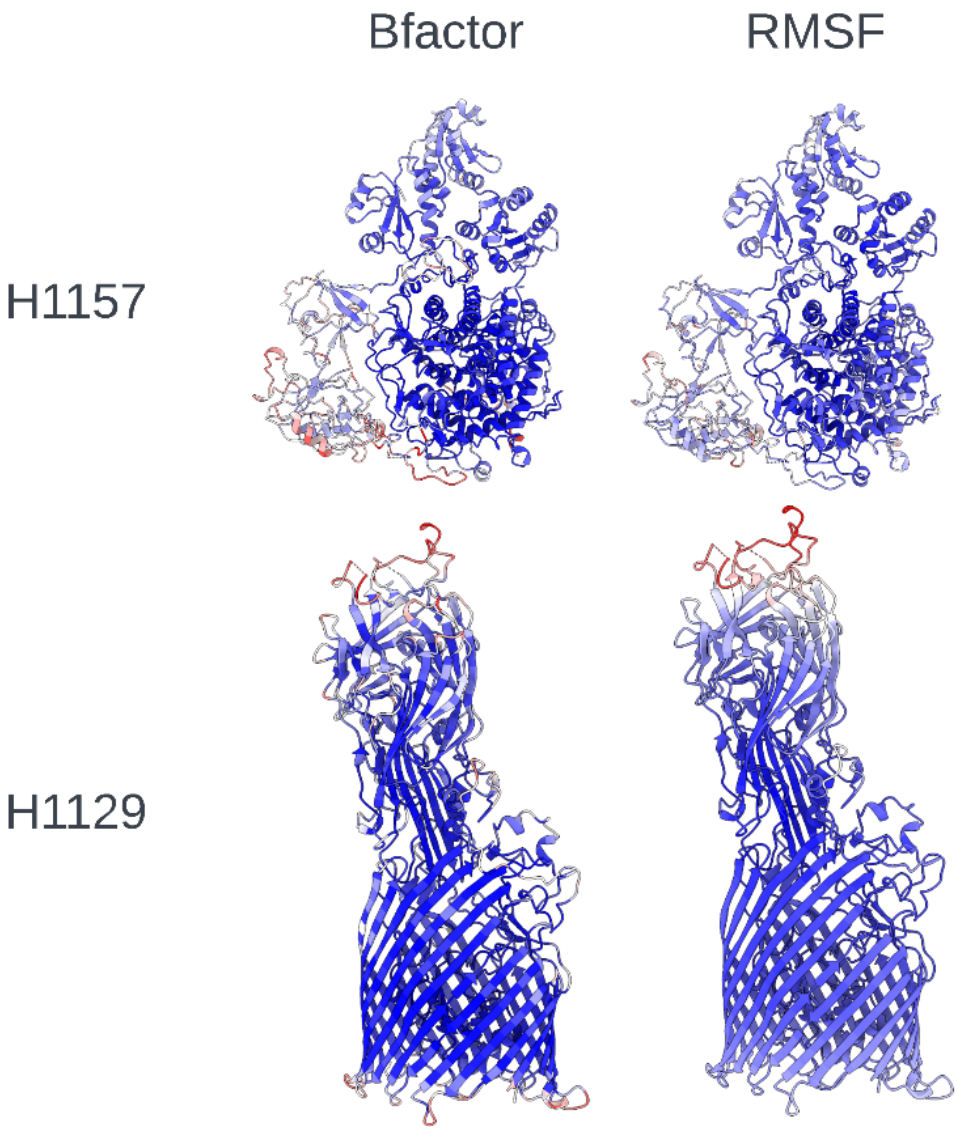

Fig. S2: Comparison of Bfactor and RMSF of best docked predictions for two cryoEM targets. H1157 had a well-resolved core with low Bfactors (dark blue) and a number of domains which were less resolved (light-blue to red) suggesting they move independently from the core. When coloured by the RMSF of the docked models one sees a similar trend. H1129 had lower resolution loops in the extremities which was also reflected by higher Bfactors. When coloured by the RMSF of the docked models, a similar pattern is seen.

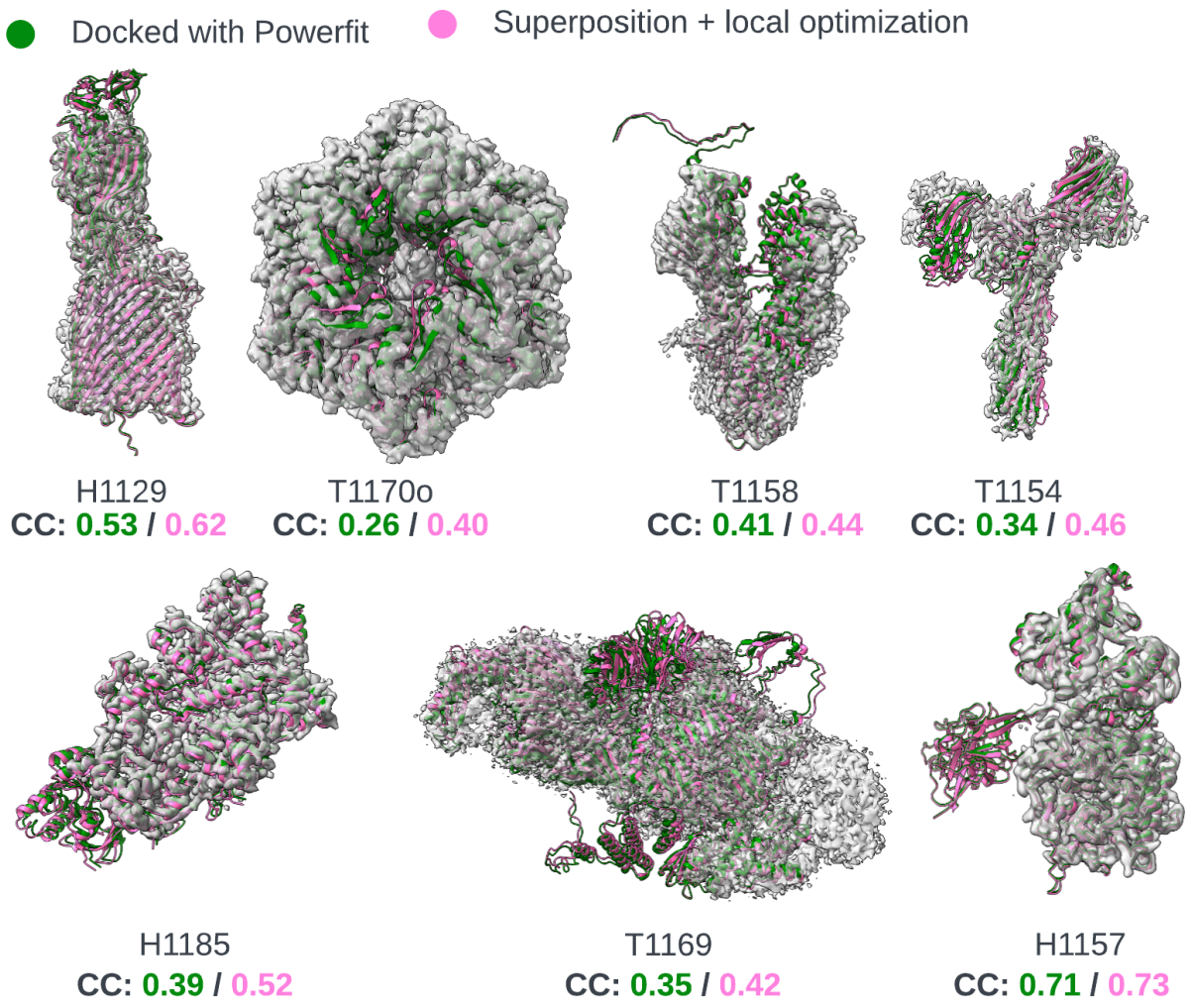

Figure S3. Comparison of the poses resulting from PowerFit model docking vs. the poses resulting from initial superposition on the reference for some of the protein targets. For each CASP target, the pose of the first-ranked model based PowerFit docking is shown (green) within the cryoEM density (grey) along the pose determined by first superposing it on the reference structure and then optimizing its fit using ChimeraX (pink). The corresponding CC scores for each fit is indicated below the target name.

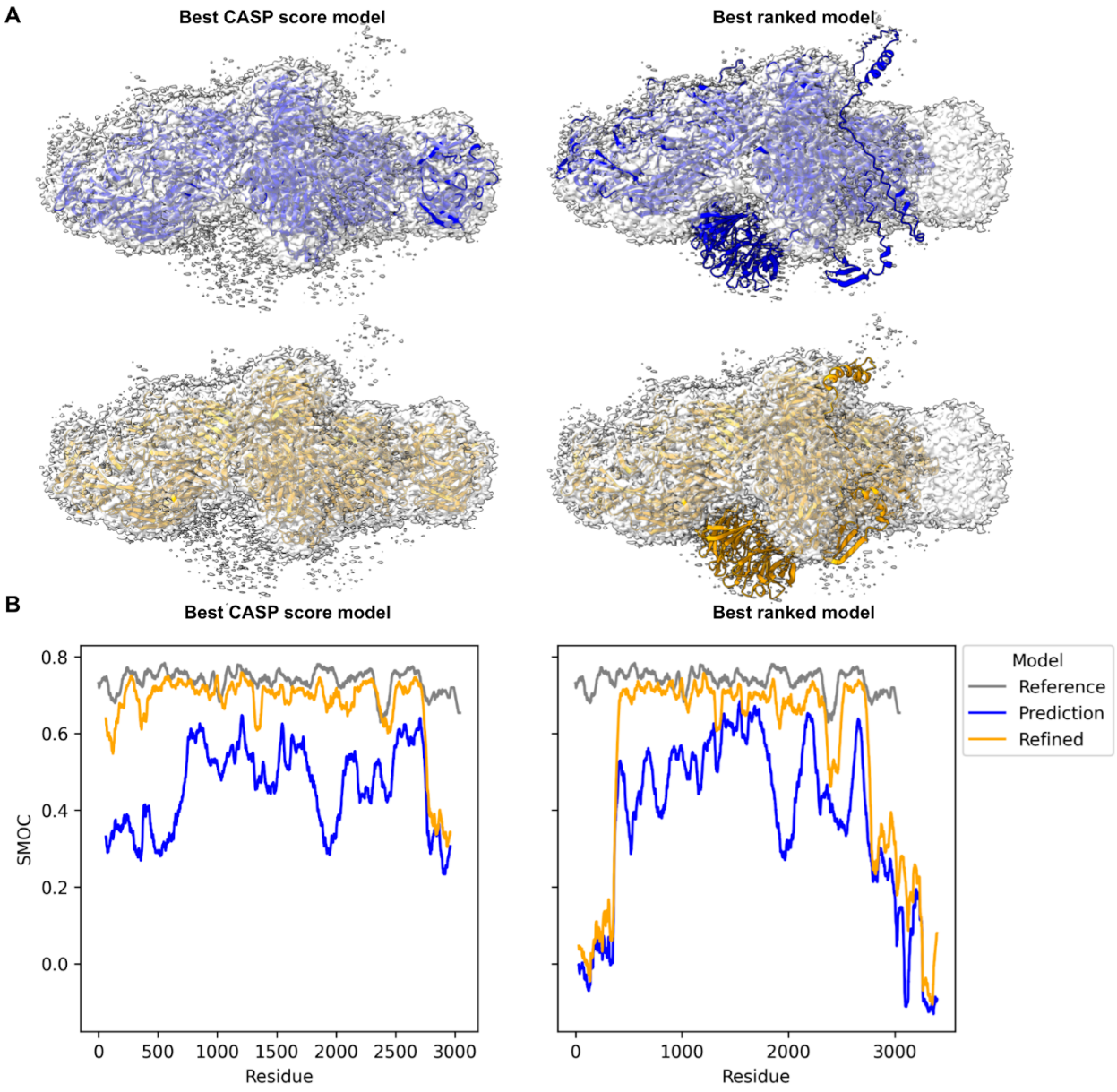

Fig. S4. Refinement of the prediction with the best CASP score from Yang (group 229) and the best ranking Shennong (group 466). In **(A)** SMOC scores of the predictions and the corresponding structures in the experimental density. Both models have several (often different) regions which fit relatively well. The best-ranked model had more C-terminal residues modeled but had a poorly placed N-terminal β-propeller domain. After refinement **(B)**, the model based on CASP metrics had higher SMOC scores overall. The poorly placed β-propeller of the best-ranked model was too distant to be refined.

Supplemental videos

Supplemental Video 1: Refinement of R1126TS287_2:
https://syncandshare.desy.de/index.php/s/kx8fTAETgiimew4
Supplemental Video 2: Refinement of R1138TS232_3 in Mature map:
https://syncandshare.desy.de/index.php/s/dXWwHEFeKoyjLF9
Supplemental Video 3: Refinement of R1138TS232_4 in Young map:
https://syncandshare.desy.de/index.php/s/CqbF3xFm5XxezTF

Supplemental References

1. Cragnolini T, Kryshtafovych A, Topf M. Cryo-EM targets in CASP14. *Proteins*. 2021;89(12):1949-1958. doi:10.1002/prot.26216

2. Kryshtafovych A, Malhotra S, Monastyrskyy B, et al. Cryo-electron microscopy targets in CASP13: Overview and evaluation of results. *Proteins*. 2019;87(12):1128-1140. doi:10.1002/prot.25817

3. Joseph AP, Malhotra S, Burnley T, et al. Refinement of atomic models in high resolution EM reconstructions using Flex-EM and local assessment. *Methods*. 2016;100:42-49. doi:10.1016/j.ymeth.2016.03.007

4. Cragnolini T, Beton J, Topf M. Cryo-EM structure and B-factor refinement with ensemble representation. *bioRxiv*. Published online June 9, 2022:2022.06.08.495259. doi:10.1101/2022.06.08.495259

5. Eastman P, Swails J, Chodera JD, et al. OpenMM 7: Rapid development of high performance algorithms for molecular dynamics. *PLoS Comput Biol*. 2017;13(7):e1005659. doi:10.1371/journal.pcbi.1005659

6. Malhotra S, Mulvaney T, Cragnolini T, et al. RIBFIND2: Identifying rigid bodies in protein and nucleic acid structures. *Nucleic Acids Res*. Published online September 6, 2023. doi:10.1093/nar/gkad721

7. Kabsch W, Sander C. Dictionary of protein secondary structure: pattern recognition of hydrogen-bonded and geometrical features. *Biopolymers*. 1983;22(12):2577-2637. doi:10.1002/bip.360221211

8. Yang H, Jossinet F, Leontis N, et al. Tools for the automatic identification and classification of RNA base pairs. *Nucleic Acids Res*. 2003;31(13):3450-3460. doi:10.1093/nar/gkg529

9. Trabuco LG, Villa E, Mitra K, Frank J, Schulten K. Flexible fitting of atomic structures into electron microscopy maps using molecular dynamics. *Structure*. 2008;16(5):673-683. doi:10.1016/j.str.2008.03.005

10. Kawabata T. Multiple subunit fitting into a low-resolution density map of a macromolecular complex using a gaussian mixture model. *Biophys J*. 2008;95(10):4643-4658. doi:10.1529/biophysj.108.137125

11. Hornak V, Abel R, Okur A, Strockbine B, Roitberg A, Simmerling C. Comparison of multiple Amber force fields and development of improved protein backbone parameters. *Proteins*. 2006;65(3):712-725. doi:10.1002/prot.21123

12. Chou FC, Sripakdeevong P, Dibrov SM, Hermann T, Das R. Correcting pervasive errors in RNA crystallography through enumerative structure prediction. *Nat Methods*. 2013;10(1):74-76. doi:10.1038/nmeth.2262

13. Leman JK, Weitzner BD, Lewis SM, et al. Macromolecular modeling and design in Rosetta: recent methods and frameworks. *Nat Methods*. 2020;17(7):665-680. doi:10.1038/s41592-020-0848-2